



Focusing Properties of Spirally Polarized Axisymmetric QBG Beams with 4pi Configurations

V. Senthil Kumar, L. Banupriya, M. Udhayakumar, K. B. Rajesh*

Department of Physics, Chikkanna Government Arts College, Tirupur, TN, India

Received: 10.12.2015 Accepted: 20.03.2016 Published: 30-03-2016

*rajeshkb@gmail.com

ABSTRACT

Tight focusing properties of spirally polarized axisymmetric QBG beam with 4pi configuration is investigated theoretically by vector diffraction theory. Calculation results show that intensity distribution in focal region can be altered considerably by beam parameter μ and spiral parameter C that indicates polarization spiral degree. By proper tuning the beam parameter and spiral parameter generate multiple focal spot. Potential application of the focal shaping technique are also discussed. The author expect such an investigation is worthwhile for optical manipulation and material processing technologies.

Keywords: Tight focusing of high NA lens; Vector diffraction theory; 4pi configuration.

1. INTRODUCTION

In optics, a tight-focusing light beam for achieving the smallest possible focal spot is an essential issue in a variety of applications where large amounts of light energy need to be confined into a small volume super-resolution scanning confocal microscopy (Dorn *et al.* 2003; Kozawa *et al.* 2011) and optical trapping (Zhang, 2010). To approach the Abbe's diffraction limit and make a breakthrough on reducing the spot size. In recent years, focusing light into a very tight spot is one of the most attractive topics in optics (Youngworth and Brown, 2000; Bokor and Davidson, 2004). The optimization of the shape and size (intensity and phase distribution) of the focal spot has been frequently discussed (Hell and Stelzer, 1992; Chen and Zhao, 2012; Wang *et al.* 2008; Wang *et al.* 2012; Li *et al.* 2012). The polarization as an important parameter of the focal field, however, does not receive enough attention. Under tightly focusing condition, the longitude component of the focal field plays an equally important role as the transverse one (Youngworth and Brown, 2000). The field characterized by three-dimensional (3D) polarization is expected to have extensional functionalities and applications (Wang *et al.* 2012; Li *et al.* 2012). In confocal microscopy it is often desired to achieve high axial as well as transverse resolution. For confocal microscopy that scans the specimen in three dimensions the ideal goal is a focal spot that has complete spherical symmetry, the smallest possible size, and minimal side lobe levels. In a 4Pi focusing system radially polarized laser beams can be focused to a spherical focal spot. The concept of 4Pi focusing is proposed to increase the numerical aperture of a focusing system (Hell and

Stelzer, 1992; Caron and Potvliege, 1999; Hricha and Belafhal, 1992). Of-late, high-throughput Nano fabrication using visible light is in demand due to the advancement in nanotechnology for enabling mass production of nano-devices. The proposed optical system consists of two cylindrical lens placed opposite to each other, making a total angle of 2π between them as shown in fig. 1. We termed this geometry as 2π and the proposed technique is termed as 2π -nano-lithography system A three-dimensional (3D) symmetrical, spherical/isotropic focal spot is advantageous in many microscopy schemes, such as confocal, stimulated emission depletion (STED), and dark field microscopy as well as for optical tweezers/particle trapping, optical storage, lithography etc. Reduction in spot size in the axial direction can be achieved by 4Pi focusing, which doubles the aperture of the focusing system by employing two opposing lenses, consequently resulting in coherent illumination from both sides. The interference process produces an intensity point spread function with a maximum main axial that is approximately four times narrower than that of a single-objective focusing system (Hricha and Belafhal, 2005). Extremely long optical chain and dark channel were observed in the 4Pi focusing of a radially polarized vortex beam (Wang and Lu, 2002). In optical trapping system, it is usually deemed that the forces exerted on the particle in light field consist of two kinds of forces, one is the optical gradient force, which play a crucial role in constructing optical trap and its intensity is proportional to the optical intensity gradient; the other kind of force is scattering force, which usually has complex forms because this kind of force is related to the properties of the trapped particles, and whose intensity is proportional to the optical intensity (Youngworth and Brown, 2000).

2. THEORY

Bessel-modulated Gaussian beams with quadratic radial dependence (QBG beam) are a novel class of beams expressed in cylindrical coordinate system. It is noted that the zeroth-order QBG beam, which is referred to as the axisymmetric QBG beam, can be expanded in Laguerre–Gauss modes and has a very flat axial profile. Fig. 1 sketches the geometry of a typical 4Pi focusing system. It consists of two objective lenses of high numerical aperture (For the simplicity of mathematic derivation, we assume that $NA = 1$). Two counter-propagating spirally polarized axisymmetric QBG light beams are focused by both lenses such that the foci coincide. In the focusing system we investigated, focusing beam is spirally polarized axisymmetric QBG beam whose value of transverse optical field is same as that of the scalar axisymmetric QBG (Ziyang Chen and Daomu Zhao, 2012; Zhan, 2009) and its polarization distribution turns on spiral (Zhan, 2009). Therefore, in the cylindrical coordinate system $(r, \phi, 0)$ the field distribution $\vec{E}(r, \phi, 0)$ of the spirally polarized axisymmetric QBG beam at the plane $z = 0$ is written as,

$$\vec{E}_0(r, \phi, z=0) = E_0(r, \phi, z=0) [\cos(\phi(r))\vec{n}_r + \sin(\phi(r))\vec{n}_\phi] \rightarrow (1)$$

Where $\phi(r)$ is the polarization angle from radial direction, and is function of radial coordinate for the spirally polarized axisymmetric- QBG beam. \vec{n}_r and \vec{n}_ϕ are the radial and azimuthally unit vectors of polarized direction of spirally polarized axisymmetric QBG beam.

$$E_0(r, \phi, z = 0) = J_0\left(\frac{\mu r^2}{\omega_0^2}\right) \exp\left(\frac{r^2}{\omega_0^2}\right) \rightarrow (2)$$

Where J_0 denotes the Bessel function of order zero, ω_0 is the waist width of the Gaussian beam, μ is a beam parameter which is complex-valued in general. After simple derivation (Hao, 2007), eq. (2) can be rewritten as,

$$E_0(r, \phi, z = 0) = J_0\left[\frac{\mu \sin^2(\theta)}{w^2 NA^2}\right] \exp\left[\frac{\sin^2(\theta)}{w^2 NA^2}\right] \rightarrow (3)$$

Parameter $w = \frac{\omega_0}{r_0}$ is called relative waist width, where

r_0 is radius of incident optical aperture. NA is numerical aperture of the focusing system. It represents the polar angle corresponding to radial coordinate r . $\phi(r)$ characterizes the polarization of focusing spirally

polarized axisymmetric QBG beam and can be expressed as:

$$\phi(\theta) = C \cdot \frac{r}{r_0} \cdot \pi = C \cdot \frac{\tan(\theta)}{\tan(\alpha)} \cdot \pi \rightarrow (4)$$

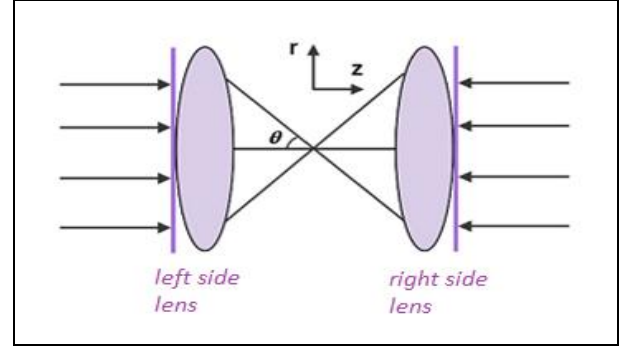


Fig. 1: Geometry of a 4Pi focusing system consisting of two confocal high-NA objectives and illuminated by two counter-propagating spirally polarized axisymmetric QBG beams

Where $\alpha = \arcsin(NA)$ is convergence angle corresponding to the radius of incident optical aperture. C is spiral parameter indicating polarization spiral degree the electric field in focal region of spirally polarized axisymmetric QBG beam is,

$$\vec{E}_1(r, \phi, z) = E_r \vec{e}_r + E_z \vec{e}_z + E_\phi \vec{e}_\phi \rightarrow (5)$$

Where \vec{e}_r , \vec{e}_z and \vec{e}_ϕ are the unit vectors in the radial, azimuthal, and propagating directions, respectively. Parameters E_r , E_z , and E_ϕ are amplitudes of the three orthogonal components and can be expressed as

$$E_r(r, z) = A \int_0^\alpha \sqrt{\cos \theta} \cdot \cos[\phi(\theta)] \cdot E_0 \sin(2\theta)$$

$$J_1(kr \sin \theta) \exp(ikz \cos \theta) d\theta \rightarrow (6)$$

$$E_z(r, z) = 2iA \int_0^\alpha \sqrt{\cos \theta} \cdot \cos[\phi(\theta)] \cdot E_0 \sin^2(\theta)$$

$$J_0(kr \sin \theta) \exp(ikz \cos \theta) d\theta \rightarrow (7)$$

$$E_\phi(r, z) = 2A \int_0^\alpha \sqrt{\cos \theta} \cdot \sin[\phi(\theta)] \cdot E_0 \sin(\theta)$$

$$J_1(kr \sin \theta) \exp(ikz \cos \theta) d\theta \rightarrow (8)$$

Where r and z are the radial and z coordinates of observation point in focal region, respectively. The optical intensity in focal region is proportional to the modulus square of eq. (5). Basing on the above equations, focusing properties of spirally polarized axisymmetric QBG beam can be investigated theoretically. Finally, the electric field near the focus of a 4Pi focusing system can be expressed as (Hao, 2007),

$$\overline{E}(r, \varphi, z) = \overline{E}_1(r, \varphi, z) + \overline{E}_2(-r, \varphi, -z)$$

Where E_1 and E_2 denote electric fields of the left and the right objectives. The schematic diagram of the optical setup for the experimental determination of the field distribution is as shown in fig. 1. A camera was placed directly near the focus of the cylindrical lens and scanned across the focal plane.

3. RESULTS & DISCUSSION

The tight focusing properties of spirally polarized QBG (Quadratic Bessel-Gaussian) beam is investigated theoretically. Fig.2 shows that a focal structure was generated for the intensity distribution in focal region for the incident spirally polarized QBG beam under the condition of $\mu=1$ and for different C values. It is observed from the fig. 2(a), when $C=0$, the generated focal structure is a focal spot FWHM of 0.201λ and focal depth of 0.402λ . Fig. 2(b) shows that two tiny focal holes generated when the value of C is increased to 0.6. The FWHM of focal holes are 0.583λ and are separated by a distance of 0.24λ .

Fig. 2(c) shows further increasing the value of C to 0.9, focal hole splits along optical axis and forms four bright spot in the focal region. Fig. 2(d) shows the new focal structure should be generated by increasing the spiral parameter $C=1.2$. Further, increasing C to 1.5 results in formation of new elongated spots along with the four bright spot. It is noted that further increasing of C results in formation of multiple spots with larger size. Fig. 2(e) represents the center of the focal structure having the weak intensity distribution in radial direction either side of two bright spot generated. Fig. 2(f), shows that further, increasing the value of $C=1.8$ two bright focal spot either side having the weak focal spot. Fig. 2(g), shows that increasing $C=2.1$ the generated focal spot splits along optical axis. Fig. 2(h), shows that the increasing value of C to 2.4, generated the new formation focal structures with the intensity distribution increasing on radial direction. Fig. 2(i), shows that increasing the value of C to 3.0, generated the bright focal spot splits along optical axis.

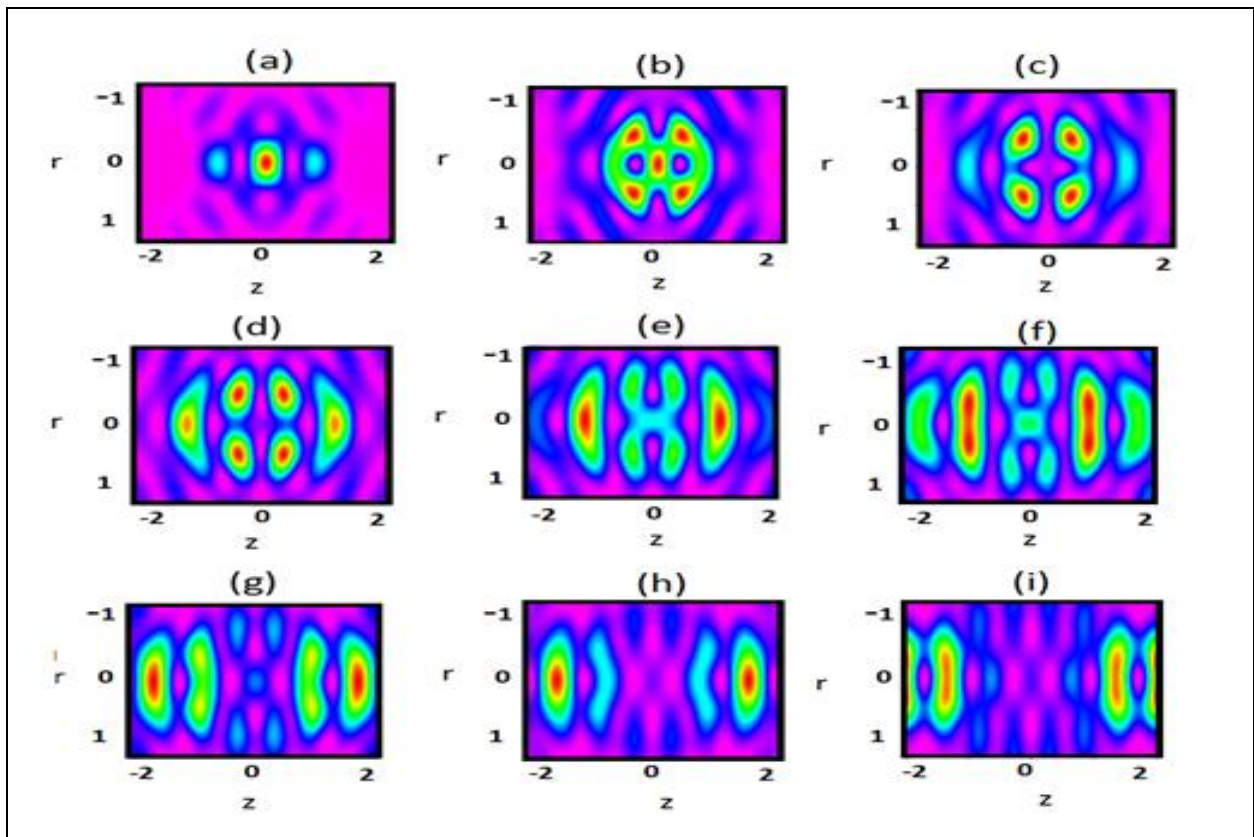


Fig. 2: Intensity distributions in focal region $\mu=1$ and (a) $C = 0$, (b) $C = 0.6$, (c) $C=0.9$, (d) $C = 1.2$, (e) $C = 1.5$, (f) $C = 1.8$, (g) $C = 2.1$, (h) $C = 2.4$, (i) $C=3.0$, respectively

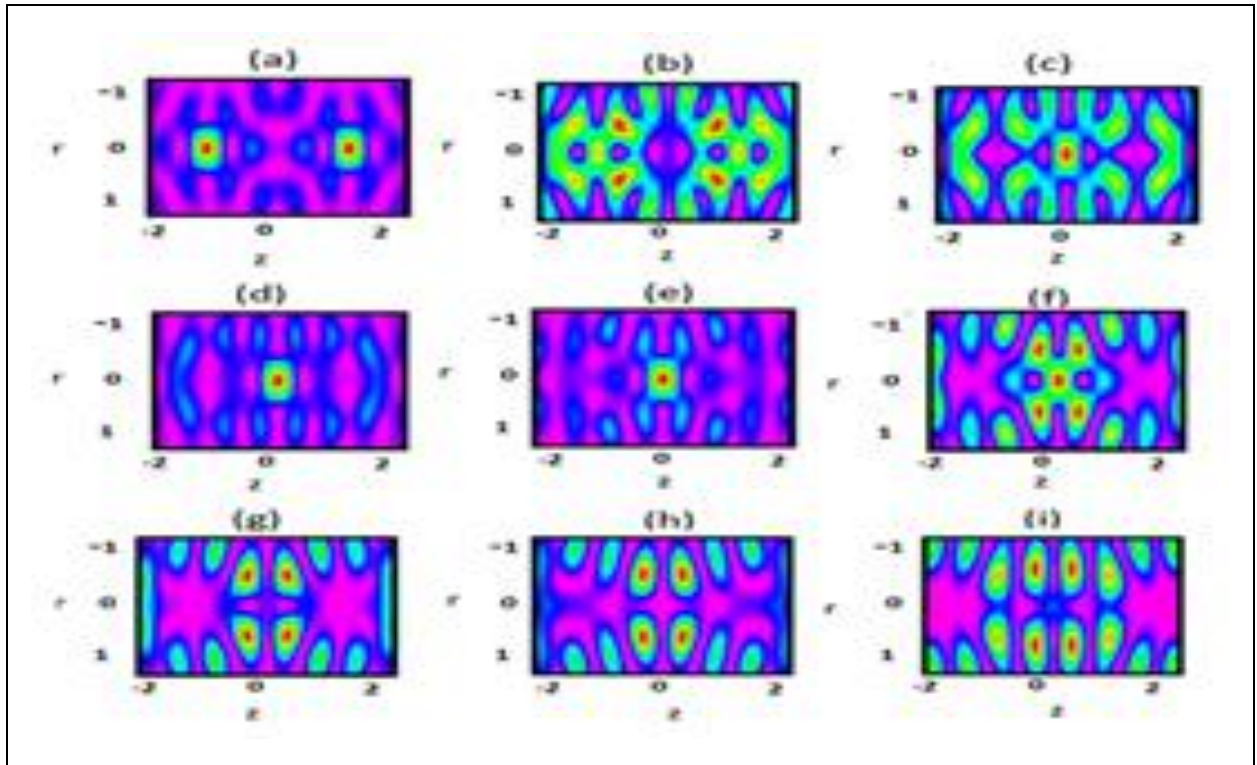


Fig. 3: Intensity distributions in focal region $\mu=4$ and (a) $C = 0$, (b) $C = 0.6$, (c) $C=0.9$, (d) $C = 1.2$, (e) $C = 1.5$, (f) $C = 1.8$, (g) $C = 2.1$, (h) $C = 2.4$, (i) $C=3.0$, respectively

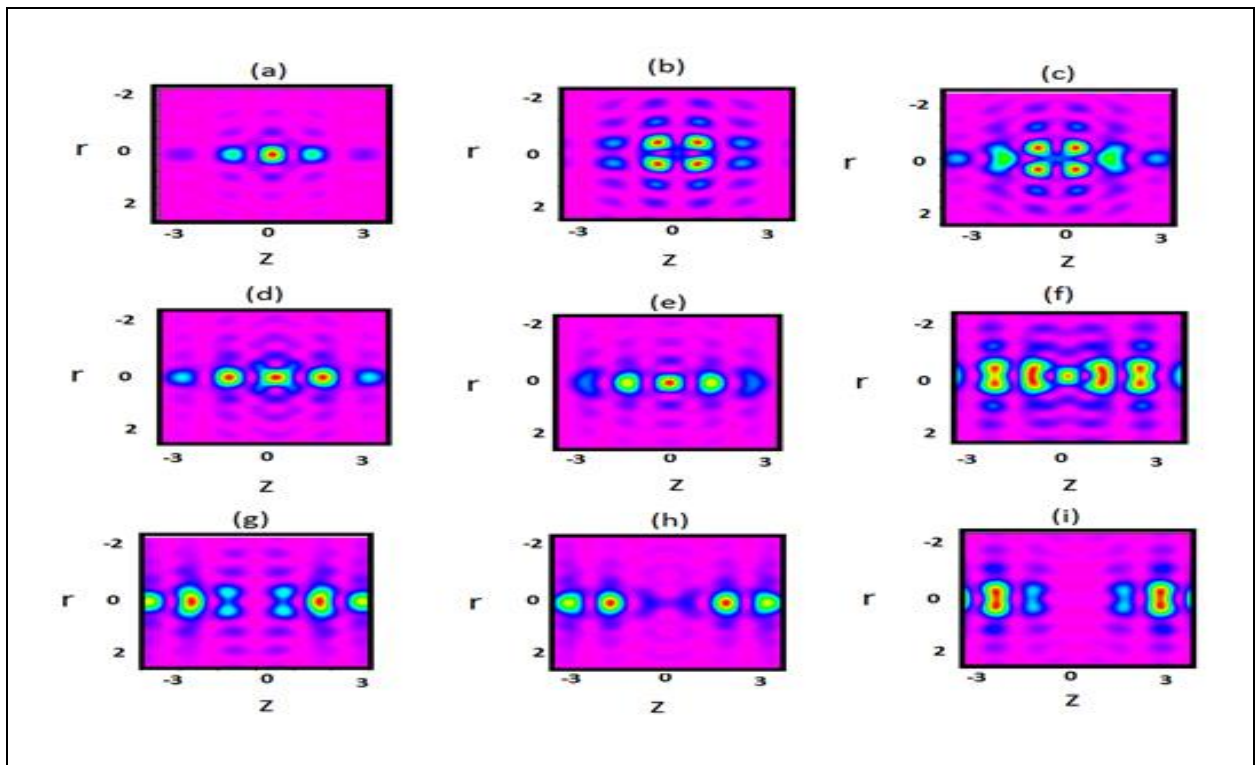


Fig. 4: Intensity distributions in focal region $\mu=5I$ and (a) $C = 0$, (b) $C = 0.6$, (c) $C=0.9$, (d) $C = 1.2$, (e) $C = 1.5$, (f) $C = 1.8$, (g) $C = 2.1$, (h) $C = 2.4$, (i) $C=3.0$, respectively

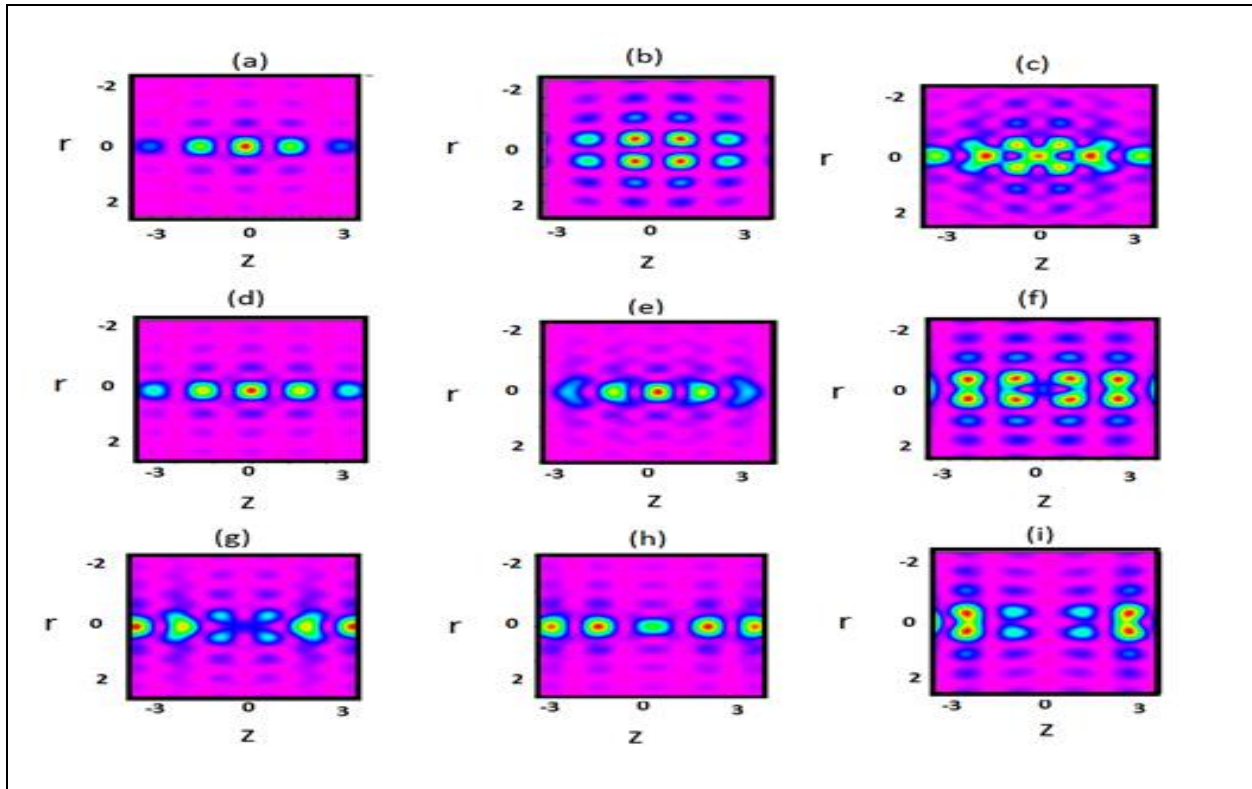


Fig. 5: Intensity distributions in focal region $\mu=10I$ and (a) $C = 0$, (b) $C = 0.6$, (c) $C=0.9$, (d) $C = 1.2$, (e) $C = 1.5$, (f) $C = 1.8$, (g) $C = 2.1$, (h) $C = 2.4$, (i) $C=3.0$, respectively

Fig. 3 shows that the focal structure generated for the intensity distribution in focal region of spirally polarized QBG beam are calculated under the condition of $\mu=4$ and the different C values. It is absorbed from fig. 3(a) when $C=0$, the resultant focal structure is a dual focal spot each having FWHM of 0.752λ and focal depth of 2.51λ . It is noted from fig. 3(b) when C is increased to 0.6 , four tiny optical bubbles are formed. Fig. 3(c) shows further increasing of C to 0.9 results in a formation of a tiny bright focal spot at the centre with radially elongated residual neighbor spots of non-uniform size. Fig. 3(d) shows when $C=1.2$, a strong focal spot with FWHM of 0.227λ , and focal depth of 0.378λ is achieved. Again increasing C to 1.5 and 1.8 , elongates the spot in the radial direction and splitted into four spots with a central bright spot as shown in fig.3(e), and fig.3(f) with FWHM 0.224λ , and 0.189λ , and focal depth of 0.448λ , and 0.524λ , respectively. Fig. 3(g) shows when $C=2.1$ splitted focal holes having FWHM of 0.334λ , and focal depth of 0.944λ is achieved. Fig. 2(g) shows for $C=2.4$, the spots elongates in the radial directions FWHM 0.766λ and focal depth of 0.874λ . Fig. 3(i) shows that for $C=3$, multiple focal holes of unequal FWHM 0.262λ , and focal depth of 0.804λ are achieved.

Fig. 4 shows same as fig.3 but for $\mu=5I$. It is noted from fig. 4(a) when $C=0$, a central bright spot with two side spot. Fig.4(b) shows that when $C=0.6$, generated the focal hole of FWHM of 0.239λ separated by a distance of 0.348λ is achieved. When $C=0.9$, four splitted focal spots is observed in fig. 4(c) the FWHM 0.204λ and focal depth is 3.26λ . When $C=1.2$, a central rectangular spot surrounded by a two spherical spot is observed in fig. 4 (d). Fig. 4(e) shows increasing C to 1.5 results in the elongation of spherical spots. Fig. 4(f) shows when $C=1.8$, further elongation of side spots is observed.

Fig. 4(g) shows increasing C to 2.1 results in the elongation of increasing the intensity on radial direction. Fig. 4(h) shows that the increasing C to 2.4 results in the two spherical bright spot and weak focal spot. Further increasing C to 3.0 results in the elongation of increasing the intensity on radial direction.

Fig. 5 shows same as fig.5 but for $\mu=10I$. It is noted when $C=0$, the results in single bright spot in fig. 5(a) with FWHM 0.185λ and focal depth of 0.592λ is absorbed. Fig. 5(b) shows that further increasing C to 0.6 generating the four bright spots and two weak spot with FWHM 0.215λ and focal depth 2.155λ . Fig. 5(c) shows

that two tiny optical bubble further increasing C to 0.9 with FWHM 0.22λ and focal depth of 3.44λ respectively. Fig.5 (d, e) shows that further increasing C to 1.2 and 1.5 central bright spot and two weak spots with FWHM 0.189λ , and 0.151λ and focal depth of 0.504λ , and 0.454λ respectively. Fig. 5(f) Shows that multiple focal structures in axial direction increasing C to 1.8. Fig. 5(g) shows that further increasing C to 2.1 generated two central weak spots. Further increasing C to 2.4 weak spot at the Centre elongation of two bright spot in side region seems to the fig. 5(h). Fig. 5(i) shows that the elongation of radial direction with in two focal spots . A multi-focal excitation technique may find potential applications in optical tweezers for trapping and manipulation of molecules. Additionally, fluorescence correlation spectroscopy can benefit from such an excitation technique. In particular, diffusion studies can be performed simultaneously on multiple sample layers and for determining molecular interactions of multiple species.

4. CONCLUSION

In this communication, we propose a multiple excitation focal structure based high resolution imaging technique. The resulting PSF is a consequence of the superposition of counter propagating spatially filtered structured wave fronts. Unlike others, the proposed optical mask has the added advantage of impressive improvement in both axial and lateral resolution. Potential applications in fluorescence spectroscopy and nano-bioimaging are anticipated.

FUNDING

This research received no specific grant from any funding agency in the public, commercial, or not-for-profit sectors.

CONFLICTS OF INTEREST

The authors declare that there is no conflict of interest.

COPYRIGHT

This article is an open access article distributed under the terms and conditions of the Creative Commons Attribution (CC-BY) license (<http://creativecommons.org/licenses/by/4.0/>).



REFERENCES

- Bokor, N. and Davidson, N., Toward a spherical spot distribution with 4π focusing of radially polarized light, *Opt. Lett.*, 29(17), 1968-1970(2004).
<https://doi.org/10.1364/OL.29.001968>
- Caron, C. F. R., Potvliege, R. M., Bessel-modulated gaussian beams with quadratic radial dependence, *Opt. Commun.*, 164(1-3), 83-93(1999).
[https://doi.org/10.1016/S0030-4018\(99\)00174-1](https://doi.org/10.1016/S0030-4018(99)00174-1)
- Chen, Z. and Zhao, D., 4π focusing of spatially modulated radially polarized vortex beams, *Opt. Lett.*, 37(8), 1286-1288(2012).
<https://doi.org/10.1364/OL.37.001286>
- Dorn, R., Quabis, S. and Leuchs, G., Sharper focus for a radially polarized light beam, *Phys. Rev. Lett.*, 91, 233901-233908 (2003).
<https://doi.org/10.1103/PhysRevLett.91.233901>
- Hao, B., Spirally in homogeneous polarization and its application in beam shaping, Dissertation at University Minnesota, 2007.
- Hell, S. and Stelzer, E. H. K., Properties of a 4π confocal fluorescence microscope, *J. Opt. Soc. Am. A.*, 9(12), 2159-2166(1992).
<https://doi.org/10.1364/JOSAA.9.002159>
- Hricha, Z. and Belafhal, A., Focal shift in the axisymmetric Bessel-modulated gaussian beam, *Opt. Commun.*, 255(4-6), 235-240(2005).
<https://doi.org/10.1016/j.optcom.2005.06.025>
- Kozawa, Y., Hibi, T., Sato, A., Horanai, H., Kurihara, M., Hashimoto, N., Yokoyama, H., Nemoto, T. and Sato, S., Creation of polarization gradients from superposition of counter propagating vector LG beams, *Opt. Express*, 19(17), 15947-15954(2011).
<https://doi.org/10.1364/OE.19.015947>
- Li, X., Lan, T. -H., Tien, C. -H. and Gu, M., Three-dimensional orientation-unlimited polarization encryption by a single optically configured vectorial beam, *Nat. Commun.*, 3, 998(2012).
<https://doi.org/10.1038/ncomms2006>
- Sick, B., Hecht, B. and Novotny, L., Orientational imaging of single molecules by annular illumination, *Phys. Rev. Lett.*, 85(21), 4482-4485(2000).
<https://doi.org/10.1103/PhysRevLett.85.4482>
- Wang, H., Shi, L., Lukyanchuk, B., Sheppard, C. and Chong, C. T., Creation of a needle of longitudinally polarized light in vacuum using binary optics, *Nat. Photonics.*, 2, 501-505(2008).
<https://doi.org/10.1038/nphoton.2008.127>

- Wang, J., Chen, W. and Zhan, Q., Creation of uniform three-dimensional optical chain through tight focusing of space-variant polarized beams, *J. Opt.*, 14(5), 055004(2012).
<https://doi.org/10.1023/A:1021160303678>
- Wang, X. and Lü, B., The beam propagation factor and far-field distribution of Bessel modulated gaussian beams, *Opt. Quant. Electron.*, 34(11), 1071-1077(2002).
<https://doi.org/10.1023/A:1021160303678>
- Youngworth, K. S. and Brown, T. G., Focusing of high numerical aperture cylindrical-vector beams, *Opt. Express*, 7(2), 77-87(2000).
<https://doi.org/10.1364/OE.7.000077>
- Zhan, Q., Cylindrical vector beams: from mathematical concepts to applications, *Adv. Opt. Photon.*, 1(1), 1-57(2009).
<https://doi.org/10.1364/AOP.1.000001>
- Zhang, Y., Suyama, T. and Ding, B., Longer axial trap distance and larger radial trap stiffness using a double-ring radially polarized beam, *Opt. Lett.*, 35, 1281-1283(2010).
<https://doi.org/10.1364/OL.35.001281>
- Ziyang Chen and Daomu Zhao, 4Pi focusing of spatially modulated radially polarized vortex beams, *Opt. Lett.*, 37(8), 1286-1288(2012).
<https://doi.org/10.1364/OL.37.001286>